

MIT Open Access Articles

Interstitial Flow Promotes the Formation of Functional Microvascular Networks In Vitro through Upregulation of Matrix Metalloproteinase#2

The MIT Faculty has made this article openly available. **Please share** how this access benefits you. Your story matters.

Citation: Zhang, Shun, Wan, Zhengpeng, Pavlou, Georgios, Zhong, Amy X, Xu, Liling et al. 2022. "Interstitial Flow Promotes the Formation of Functional Microvascular Networks In Vitro through Upregulation of Matrix Metalloproteinase#2." Advanced Functional Materials.

As Published: 10.1002/adfm.202206767

Publisher: Wiley

Persistent URL: <https://hdl.handle.net/1721.1/145456>

Version: Final published version: final published article, as it appeared in a journal, conference proceedings, or other formally published context

Terms of use: Creative Commons Attribution 4.0 International license



Interstitial Flow Promotes the Formation of Functional Microvascular Networks In Vitro through Upregulation of Matrix Metalloproteinase-2

Shun Zhang, Zhengpeng Wan, Georgios Pavlou, Amy X. Zhong, Liling Xu, and Roger D. Kamm*

Self-organized microvascular networks (MVNs) have become key to the development of many microphysiological models. However, the self-organizing nature of this process combined with variations between types or batches of endothelial cells (ECs) often lead to inconsistency or failure to form functional MVNs. Because interstitial flow (IF) has been reported to play a beneficial role in angiogenesis, vasculogenesis, and 3D capillary morphogenesis, the role IF plays during neovessel formation in a customized single-channel microfluidic chip for which IF has been fully characterized is systematically investigated. Compared to static conditions, MVNs formed under IF have higher vessel density and diameters and greater network perfusability. Through a series of inhibitory experiments, this study demonstrates that IF treatment improves vasculogenesis by ECs through upregulation of matrix metalloproteinase-2 (MMP-2). This study then successfully implements a novel strategy involving the interplay between IF and MMP-2 inhibitor to regulate morphological parameters of the self-organized MVNs, with vascular permeability and perfusability well maintained. The revealed mechanism and proposed methodology are further validated with a brain MVN model. The findings and methods have the potential to be widely utilized to boost the development of various organotypic MVNs and can be incorporated into related bioengineering applications where perfusable vasculature is desired.

1. Introduction

Recent decades have witnessed an explosive growth in the number and variety of engineered microvascular networks (MVNs). Functional vasculature is critical for the development of many microphysiological models and for diverse applications in tissue engineering. Although a vasculature plays many important roles beyond just serving as conduits, its major function is to transport nutrients, oxygen, metabolic wastes, and various cells. Lacking a perfusable vasculature hinders the advancement of numerous key techniques in bioengineering. One particular example is organoid technology. Without a perfusable vasculature, organoids in 3D culture rely solely on passive diffusion to exchange nutrients, oxygen and metabolic waste, and gradually leads to a necrotic core.^[1]


Tremendous efforts have been made to construct functional vasculature in vitro within various hydrogels with associated microfluidic chips. Many of those were

designed following a self-organizing approach, which draws upon natural self-organization and self-assembly principles by promoting conditions in which vasculogenesis or angiogenesis, two major ways of forming and developing vascularization in vivo, can occur.^[2–4] The major advantage of the self-organizing method is its similarity to the in vivo processes to grow and develop vasculature, thus leading to spontaneous formation of vessels mimicking in vivo capillaries in both function and morphology. However, inconsistencies in the self-organizing nature and the cells in their ability to form functional MVNs hinder its wider application and limit broader impact. Currently, perfusable MVNs have been constructed using multiple different combinations of primary endothelial and stromal cells, but with wide diversity of morphology and functionality. Although various methods have been proposed to reduce this variability, including standardization of cell sources using induced pluripotent stem cells (iPSC) or immortalized cells, improved seeding strategies, or identifying key growth factors in neovessel formation,^[5,6] an easily applicable approach that can effectively boost the vasculogenesis ability of endothelial

S. Zhang, Z. Wan, G. Pavlou, A. X. Zhong, R. D. Kamm
Department of Biological Engineering
Massachusetts Institute of Technology
Cambridge, MA 02139, USA
E-mail: rdkamm@mit.edu

L. Xu
Ragon institute of MGH
MIT and Harvard
Cambridge, MA 02139, USA

R. D. Kamm
Department of Mechanical Engineering
Massachusetts Institute of Technology
Cambridge, MA 02139, USA

 The ORCID identification number(s) for the author(s) of this article can be found under <https://doi.org/10.1002/adfm.202206767>.

© 2022 The Authors. Advanced Functional Materials published by Wiley-VCH GmbH. This is an open access article under the terms of the Creative Commons Attribution License, which permits use, distribution and reproduction in any medium, provided the original work is properly cited.

DOI: 10.1002/adfm.202206767

cells (ECs) and aid the robust formation of functional MVNs is still an urgent unmet need for the community.

A developing vasculature *in vivo* is subjected to various mechanical cues that were not incorporated in most *in vitro* MVN models, notably the shear stresses induced by pulsatile or unidirectional blood flow, transmural flow, and interstitial flow (IF).^[7,8] Particularly, IF plays a critical role during vasculogenesis to drive nutrients, remove metabolic wastes, and provide mechanical cues to cells, before a perfusable vasculature is established. Various microfluidic platforms have been engineered to investigate the effects of IF on ECs and vessel formation. Most of the work reported a beneficial role of IF on angiogenesis, vasculogenesis, and 3D capillary morphogenesis *in vitro*.^[9–14] These previous reports suggest that IF could be potentially used to benefit the formation of self-organized MVNs, which is validated recently by studies using generic MVNs formed with human umbilical vein endothelial cells (HUVECs) and human lung fibroblasts (HLFs) coculture,^[15] and brain MVNs with triculture of primary human brain endothelial cells (BECs), pericytes (PCs), and astrocytes (ACs).^[16] However, those studies failed to maintain a relatively stable IF during neovessel formation, and did not investigate the effects of varied IF speeds. Moreover, the underlying mechanisms by which IF lead to a better vasculature were not examined.

In this work, MVNs were grown under various physiologically relevant IF in customized single-channel microfluidic chip, for which IF was fully characterized by computation and experiments. After systematically investigating the beneficial role of IF in neovessel formation, we further demonstrated that MVN morphologies are determined by global IF rather than local IF with a modified single-channel device. Moreover, with a series of inhibitory experiments, we found that the boosted vasculogenesis capacity of ECs is associated with upregulated MMP-2 when cultured under IF. Based on the postulated mechanism, we developed a novel and robust approach to regulate key morphological parameters of self-organized MVNs through the interplay between IF and MMP-2 inhibitor, with vascular permeability and perfusability well maintained. Our findings are further validated with a BBB model made of BECs, PCs, ACs, suggesting the identified mechanism and proposed methodology could be more generally useful to ECs and have the potential to be broadly employed for numerous applications, especially to boost formation of various functional organotypic MVNs.

2. Results

2.1. In Vitro Microvascular Network Formation under IF

To investigate vessel formation under IF, two types of microfluidic device were fabricated. A common three-channel device was used to culture MVNs statically (Figure 1a) while a different device with a single rectangular gel region was fabricated to culture MVNs under IF (Figure 1b). A pressure difference was established using different levels of culture medium in the reservoirs inserted at the inlet and outlet to drive IF through the entire gel region. Through Darcy's law, we can measure matrix permeability from the rate at which liquid accumulates

in the outlet reservoir due to the pressure-driven flow (detailed analytical calculation can be found in the Supporting Information). In the single-channel device, IF can be maintained for 24 h, at which time culture medium was replenished to restore the pressure gradient. The relatively stable IF speed was confirmed with $\frac{v_{IF}(t=24h)}{v_{IF}(t=0)} = 74.6\%$ using analytical solutions

(Figure 1c) and measured matrix permeability (Figure 1d).

To ensure fibrin gel stability and identify any changes in gel properties due to flow alone, an initial set of experiments were conducted at pressure differences of 10, 20, and 30 mm H₂O applied to acellular fibrin gel in the device for 6 d. Average IF speeds of 1–3 $\mu\text{m s}^{-1}$, consistent with normal physiological ranges observed *in vivo*,^[17] were calculated from the volume of accumulated culture medium in the outlet reservoir each day. We found acellular fibrin gels to be stable under our experimental conditions for at least 6 d. Furthermore, the measured IF speeds agree well with our analytical calculation (Figure 1e).

Next, we seeded HUVECs with HLFs in microfluidic devices to form MVNs. IFs were induced with 10, 20, and 30 mm height differences of culture medium between the inlet and outlet. In the first 24 h, different pressure gradients lead to distinct IF speeds (Figure 1f), and the measured average IF speeds agree well with the IF speeds in acellular fibrin gel, suggesting that the embedded cells did not alter matrix permeability when initially seeded. However, as the cells self-organize into MVNs and remodel the extracellular matrix (ECM), the effective matrix permeability drastically changed. Interestingly, the effective matrix permeability continued to decrease over the first 3 d (Figure 1g), likely due to a combination of cell-secreted ECM and matrix remodeling by HUVECs and HLFs. After this initial period, as the nascent vessels progressively connected with each other and the MVNs become gradually perfusable, luminal flow dominated over IF and equilibrated the restored pressure difference in only a few hours so it was no longer possible to measure matrix permeability. At day 6, ECs self-organized into densely connected 3D MVNs mimicking the morphology of *in vivo* capillaries. A fully perfusable MVN formed across the gel region over the entire length of 15 mm, as confirmed by perfusing dextran from the inlet (Figure 1h).

2.2. IF Improves the Formation of Functional MVNs

To systematically investigate the effect of IF on vasculogenesis *in vitro*, HUVECs and HLFs were cocultured in the fibrin gel under static and various IF conditions. By day 6, when MVNs were interconnected and perfusable, clear morphological differences could already be observed in projected images acquired in devices cultured under static and various IF conditions (Figure 2a). Our quantification clearly showed that vessel morphology was noticeably affected by IF treatment.^[18] MVNs formed under IF covered significantly more projected area with perfusable vessels. Interestingly, the largest perfusable vessel coverage occurred when subjected to low IF, and kept decreasing as IF was increased (Figure 2c). We also observed fewer branch points and longer branch length as IF

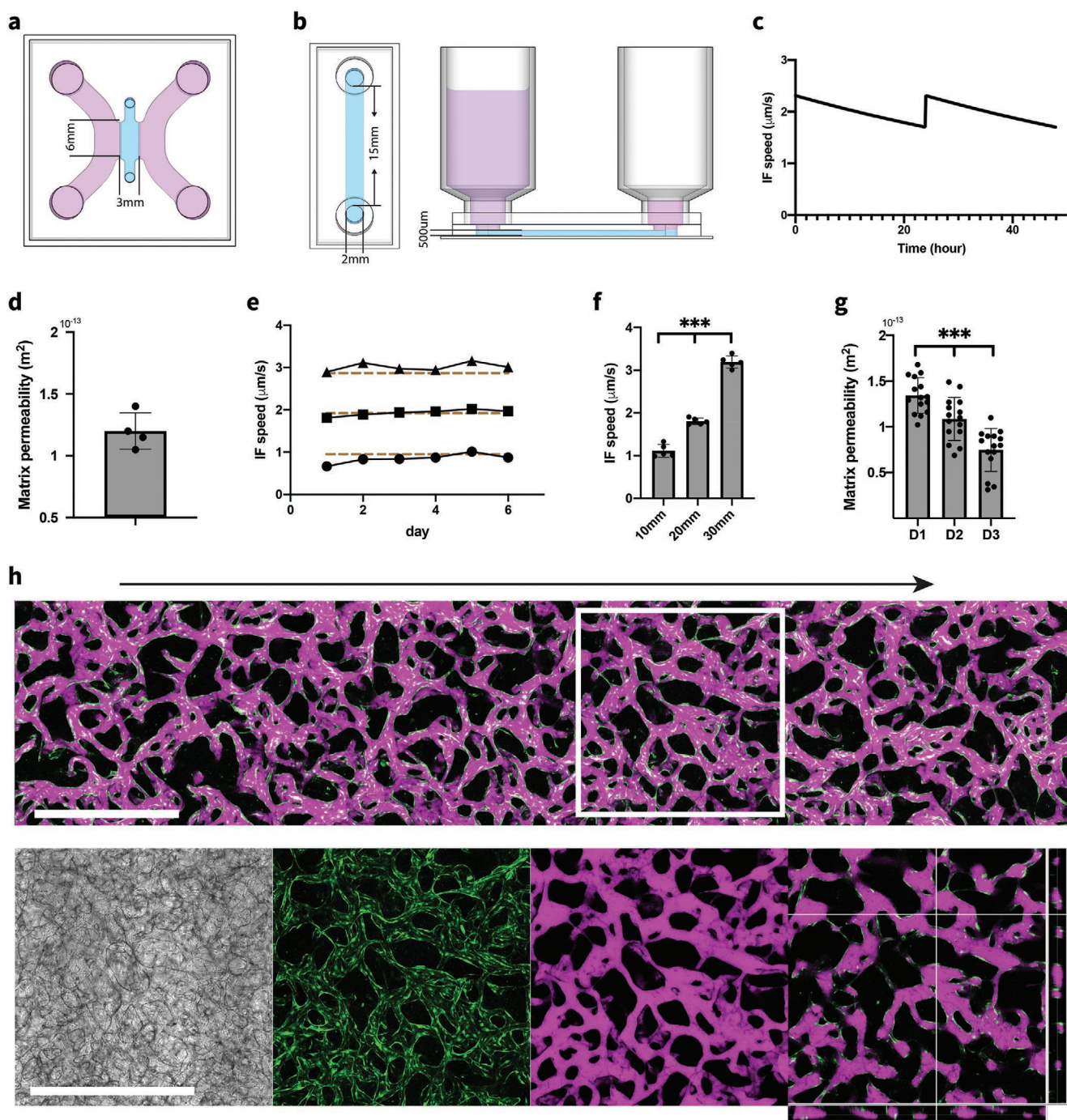


Figure 1. Microfluidic device supports formation of in vivo like MVNs during IF. a) Schematic diagram of a three-channel microfluidic device for culturing MVNs statically. b) Schematics of experimental setup to maintain IF using a single-channel device with affixed syringes. c) Time evolution of IF speed under 20 mm H₂O pressure difference, computed with analytical solution and measured matrix permeability of acellular fibrin gel. Computed IF speed decreased over time but was restored by replenishing the culture medium at 24 h intervals. d) Measurements of matrix permeability of acellular fibrin gel. $n = 5$. e) Average IF speed within acellular fibrin gel measured under 10, 20, and 30 mm H₂O pressure differences. Dashed lines correspond to calculated average IF speed with analytical solution. f) Average IF speed of the first 24 h after HUVECs and HLFs mixture seeded in devices under various pressure differences. $n = 5$ devices for each IF condition. Significance determined by t -tests. $***P < 0.01$. g) Matrix permeability measured daily during the first 3 d after HUVECs and HLFs mixture seeded in devices. $n = 15$ devices. h) Confocal projected z-stack of perfusable MVNs formed after 6 d culturing under IF generated by 20 mm H₂O pressure difference. Arrow indicates direction of IF. Green: GFP HUVECs, magenta: 40 kDa Texas Red dextran. Zoomed-in views show MVNs in the white square with separated bright field, GFP HUVECs, Texas Red dextran and cross-sectional view, respectively. Scale bar is 1 mm.

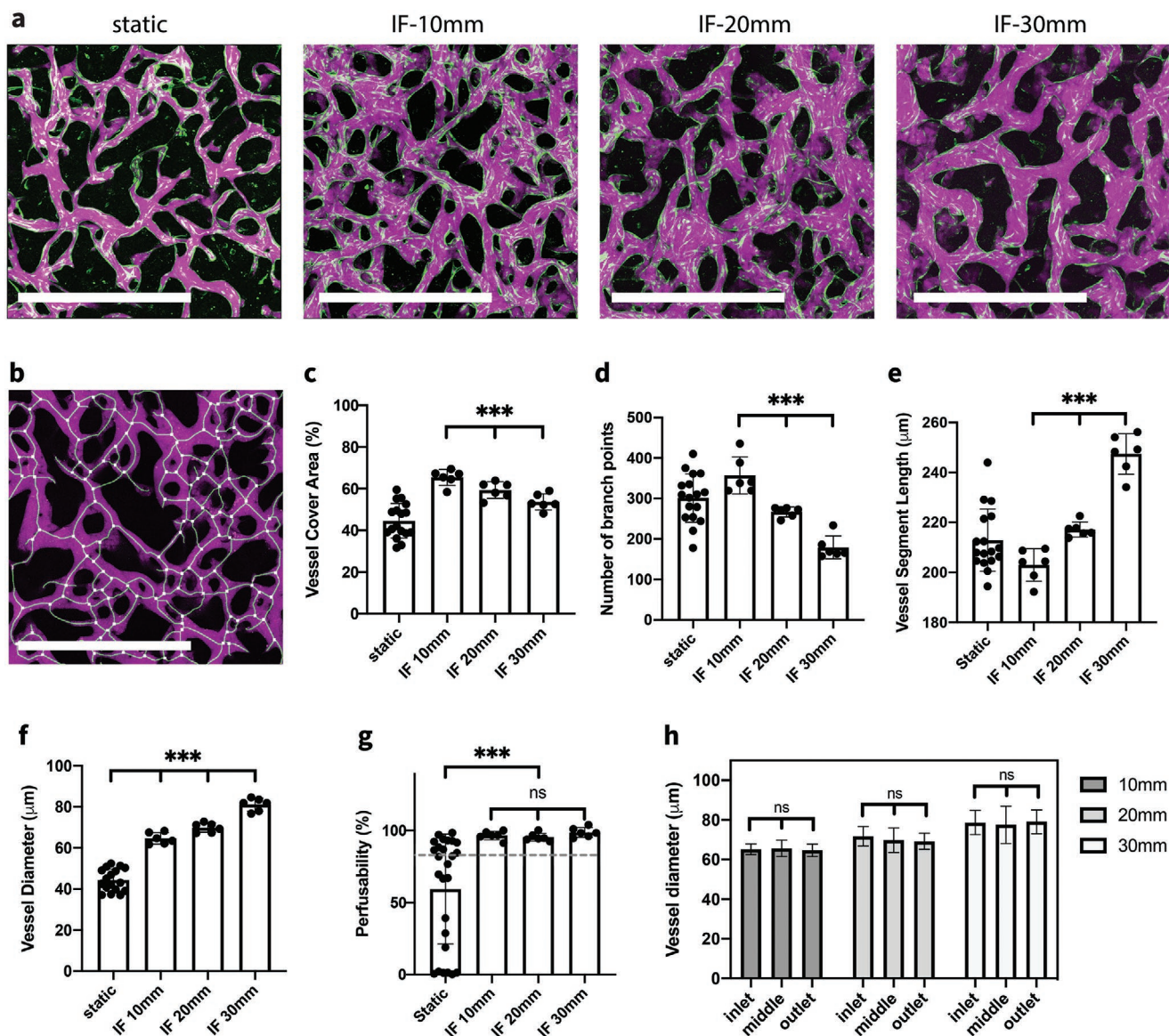


Figure 2. IF boosts the formation of functional MVNs. a) Representative images of perfusable MVNs formed statically and under various IF induced by 10, 20, and 30 mm H₂O pressure differences cultured for 6 d. Green: GFP HUVECs, magenta: 40 kDa Texas Red dextran. Scale bar is 1 mm. b) Perfusable vessel skeleton and junction points detected using fluorescent image acquired for dextran. c–f) Statistical analysis of morphological parameters of perfusable vessels cultured under various IF speed. $n = 17$ devices for static condition, $n = 6$ devices for each IF condition. Significance was calculated with t -tests. $***P < 0.01$. g) Perfusability of MVNs formed under various IF speeds; gray dashed line indicates 80% perfusability. $n = 26$ devices for static condition, $n = 6$ devices for each IF condition. h) Diameters of perfusable vessels in the inlet, middle, outlet region of MVNs formed in single-channel devices under various IF conditions. $n = 4$ devices for each IF condition.

increased (Figure 2d,e). Vessel diameters were strongly affected by IF, in comparison to MVNs formed statically. IF treatment led to vessels with significantly larger diameters (Figure 2f). Furthermore, stronger IF engendered MVNs with significantly larger vessel diameters compared to lower IF rates.

Perfusability is one crucial factor when evaluating the quality of engineered MVNs. Usually vessels with larger diameter are easier to perfuse, so it is not surprising to find MVNs with IF treatment exhibited an overall higher perfusability. To better interpret perfusability, we defined MVNs with perfusability greater than 80% as fully perfusable, and MVNs that are not

fully perfusable but with at least one perfusable vessel across the gel region as partially perfusable. When cultured under static conditions, we find only 50% of MVNs are fully perfusable and 27% are partially perfusable. In contrast, IF substantially boosted perfusability of MVNs, with all of them fully perfusable under any of the IF conditions (Figure 2g). It also should be noted that forming perfusable vessels in the single-channel device is more challenging because patent lumens must be connected across the entire gel region, over 15 mm, while perfusable vessels only need to be connected over the width of 3 mm across gel region when cultured statically in the three-channel device.

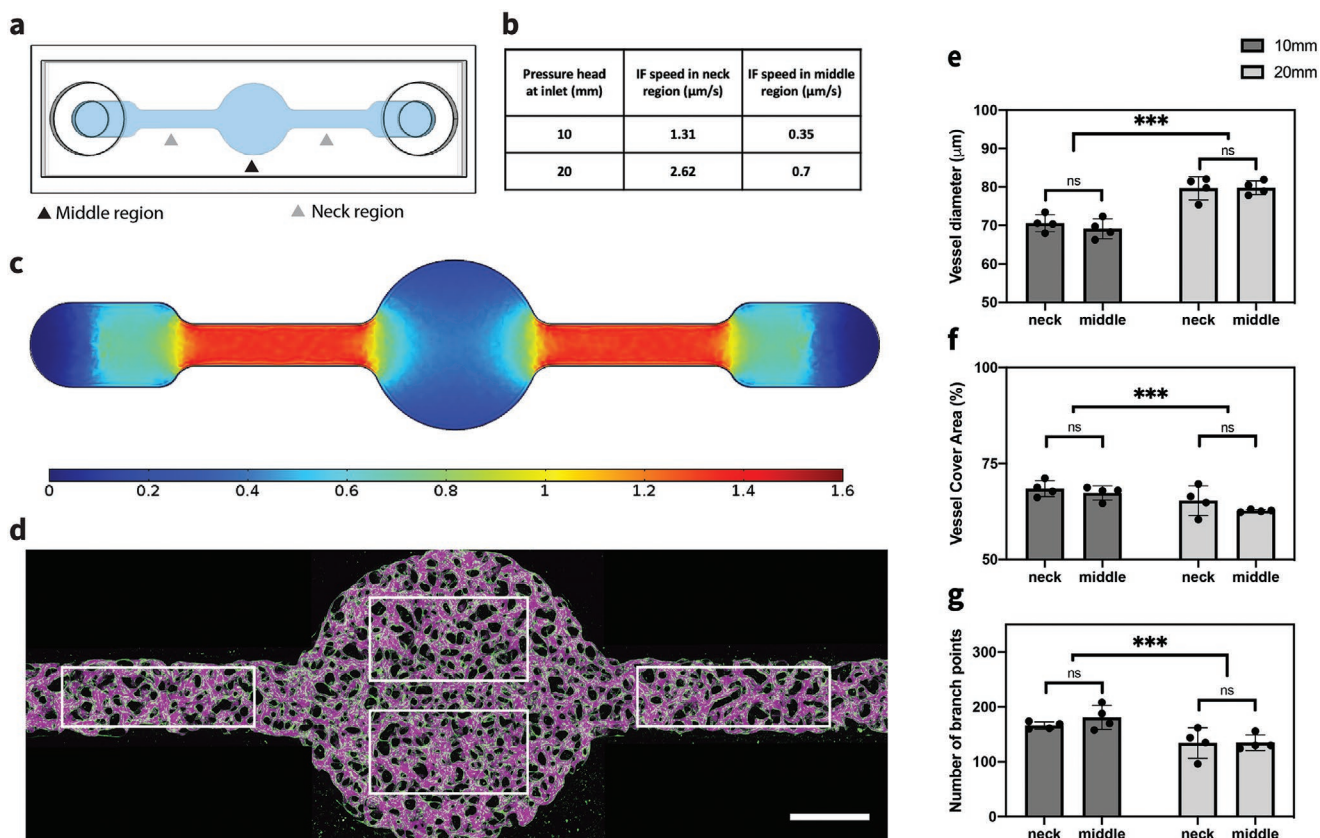


Figure 3. IF affects global MVNs structures. a) Schematic of modified single-channel device used to generate an inhomogeneous IF. b) Average IF speed in neck or middle ROIs of modified single-channel device with corresponding pressure differences, calculated in COMSOL. c) Profile of IF speed induced by 10 mm H₂O pressure difference, calculated in COMSOL. d) MVN formed under 10 mm H₂O pressure difference. White rectangles indicate ROIs of neck and middle regions for statistical analysis. Scale bar is 1 mm. e–g) Statistical analysis of morphological parameters of MVNs in middle or neck regions of modified single-channel device under 10 or 20 mm H₂O pressure difference. $n = 2$ devices for each IF condition, four ROIs in each device (two in the neck regions and two in the middle region, as shown in (d)). Significance was determined with *t*-tests. *** $P < 0.01$.

In our single-channel device, nutrients are progressively consumed by cells as the IF passes along the gel region. If the gel region is excessively long, we anticipate that at some point the medium will fail to support the formation of functional MVNs near the downstream end due to depletion of nutrients. To determine whether MVNs formed in our single-channel device were affected by nutrient depletion, we quantified the morphology at inlet, middle, and outlet region separately under various IF conditions (Figure S1, Supporting Information). We found similar morphologies in different regions when cultured under certain IF condition (Figure 2h), indicating adequate nutrients were supplied for MVNs formation over the entire gel region in our experimental setup.

Overall, MVNs formed under IF exhibited distinct morphologies with a larger projected areas and larger vessel diameters, compared with MVNs grown statically. Furthermore, the variability seemed to be greatly reduced for all morphological parameters quantified in IF cases, indicating that IF regulates the in vitro neovessel formation in a robust and replicable manner. Moreover, IF treatment significantly boosted the perfusability of self-organized MVNs, leading to a robust method of forming fully perfusable MVNs in vitro.

2.3. IF Affects Global MVN Structures within Microfluidic Device

To better understand the role IF plays during neovessel formation, we fabricated another single-channel device with a large circular middle region and two narrow neck regions (Figure 3a). With the same setup of reservoirs as before to maintain a pressure gradient along the hydrogel, we were able to generate inhomogeneous IF within the gel. Setting matrix permeability as the value we measured for acellular fibrin gel in this study, we computed the distribution of IF within the entire device using COMSOL (Figure 3c). Four regions each with the same area were chosen as ROIs, shown as white rectangles in Figure 3d. Average IF speed in each ROI was calculated under either 10 mm (100 Pa) or 20 mm (200 Pa) H₂O pressure difference; IF speed in the neck ROIs was about three times higher than the speed in middle ROI (Figure 3b). However, despite the different flow speeds, quantification did not reveal any clear differences in perfusable vessel diameters, coverage area or number of branches between the neck and middle ROIs within devices under the same pressure difference (Figure 3e–g), suggesting that MVNs were formed with relatively uniform

morphology. Distinct MVN morphologies between 100 and 200 Pa pressure difference were still obvious though, following the same trend as we reported in the previous section: MVNs formed under stronger IF were associated with larger vessels, smaller coverage area and fewer branches.

We further examined the effect of local IF on morphology. Interestingly, we observed MVNs in the neck region subjected to 100 Pa end-to-end pressure (higher local IF speed) were associated with narrower vessels, larger coverage area and more branch points compared to the MVNs in the middle region subjected to 200 Pa end-to-end pressure (lower local IF speed), which is opposite to what we found before. These findings suggest that MVN morphologies are determined by global IF rather than local IF. One possible explanation is that the secretomes of the ECs that we find are regulated by IF and are crucial for neovessel formation. Secreted factors therefore would exert their influence globally as they are transported by IF and diffusion. This knowledge is particularly important for microfluidic designs incorporating IF to boost MVN formation. Even aiming for engineering MVNs with uniform morphology, there is no need to require that the design accommodate for spatial homogeneity of IF.

2.4. IF Enhances the Vasculogenesis Capacity of EC through Upregulation of MMP-2

In order to self-organize into functional MVNs, ECs must remodel the surrounding ECM, mostly through cleavage of ECM components by secreted enzymes from embedded cells. Since we consistently observed larger diameter vessels in MVNs formed under IF, we hypothesized that IF elevates the production of proteases, thus enhancing the vasculogenesis capacity of ECs. In our systems, however, HLFs were also seeded as supporting cells with HUVECs, making it difficult to decouple the effect of IF on each cell type. We therefore decided to eliminate the HLFs from the system and test protease function using a monoculture of HUVECs to form MVNs. In our experience, only rarely are HUVECs able to self-organize into perfusable MVNs in the absence of supporting cells. And even in those rare instances in which they do, the vessels tend to be leaky and regress rapidly.^[2,3,19] Consistent with those earlier findings, when we seeded HUVECs alone in our three-channel device cultured without IF, we could find no perfusable vessels. Even though ECs seemed to form a connected network, they were not able to form continuous patent lumens (Figure 4a). In contrast, a HUVEC monoculture of the same concentration seeded in a single-channel device subjected to IF exhibited significant improvement in neovessel development. IF drastically altered the behavior of HUVECs seeded in the device, leading to robust formation of fully perfusable and interconnected MVNs by day 5 (Figure 4b).

To reveal the underlying mechanism, we performed quantitative PCR to evaluate gene expression levels in HUVECs extracted from the hydrogel at day 2 during neovessel formation cultured under both static and IF conditions. Following our hypothesis, we further carried out a series of protease inhibitory experiments to identify the specific enzymes that are responsible for the significant difference induced by IF

treatment (Figure 4c). Since fibrin was used as our 3D gel scaffold in this study, we initially focused on plasminogen activator (PA)–plasmin system because it constitutes the most common pathway for fibrinolysis. Tissue plasminogen activator (tPA) and urokinase (uPA) are two factors that convert plasminogen to active plasmin, which is the protease mainly responsible for fibrinolysis. However, we did not find clear upregulation of the PA–plasmin system when we quantified expression levels of several related genes (PLAT, PLAU, PLAU, SERPINE1, ANXA2, S100A10, THBD) (Figure 4d). Moreover, supplementing culture medium with high concentration plasminogen activator inhibitor-1 (inhibiting both uPA and tPA) or aprotinin (inhibiting plasmin) did not adversely affect the development of fully perfusable MVNs by HUVEC monoculture under IF conditions. Those findings clearly suggest that HUVECs remodel fibrin gel during neovessel formation in a plasmin-independent manner in our experimental setup, and that there must be other protease pathways mediated by IF that regulate fibrinolysis during vasculogenesis.

MMP is another common protease family consisting of more than 20 members, each of which exhibits substrate specificity for numerous ECMs. Although not specifically functioning as fibrinolytic enzymes, it has been reported that several MMPs, including at least MMP-1, MMP-2, MMP-3, and MMP-14, have the capacity to degrade fibrin gel.^[20,21] Furthermore, consistent with our finding, other groups reported that ECs invade fibrin ECM in a plasmin-independent manner and require the activity of MMPs.^[20,22,23] To confirm that MMP activity facilitates neovessel formation in a fibrin scaffold, we grew HUVEC monocultures under IF in our system adding 50×10^{-6} M marimast, a highly potent broad spectrum MMP inhibitor, to the medium. We found that inhibition of MMPs completely disrupted the vessel formation process. Even after 5 d of culturing with IF, HUVECs were only able to form short discontinuous segments with no signs of lumen formation. ECs are known to produce multiple MMPs, including MMP-1, MMP-2, MMP-9, MMP-13, MMP-14, but with variations in species and micro-environment.^[24] To identify specific MMPs that are crucial for vessel formation, quantitative PCR was performed on a series of MMPs from HUVECs cultured in 3D fibrin gel under static or IF conditions at day 2, and found that IF upregulated expression levels of MMP-1 and MMP-2 by 1.6- and 2.7-fold, respectively. MMP-14, also known as membrane type-1 MMP or MT1-MMP, was downregulated by IF (Figure 4d). However, we still included MMP-14 in the subsequent inhibitory experiments because MMP-14 has been reported to be involved in the processes of EC invasion and network formation through localized basement membrane degradation.^[21]

In our following inhibitory tests, ARP-100 (IC₅₀ values are 12, 200, 4500, >50 000, and >50 000 $\times 10^{-9}$ M for MMP-2, MMP-9, MMP-3, MMP-1, MMP-7, respectively) and NSC 405020 (selective inhibitor of proteolytic activity of MMP-14 without affecting the catalytic activity of cellular MMP-14) were used as specific inhibitors for MMP-2 and MMP-14. Because narrow band inhibitors with exclusive specificity for MMP-1 are not available at this time, we used high concentration anti-MMP-1 neutralizing antibody to inhibit its activity. Our experiments showed that blocking activity of MMP-1 does not affect vasculogenesis of HUVEC monoculture in fibrin gel under IF; fully

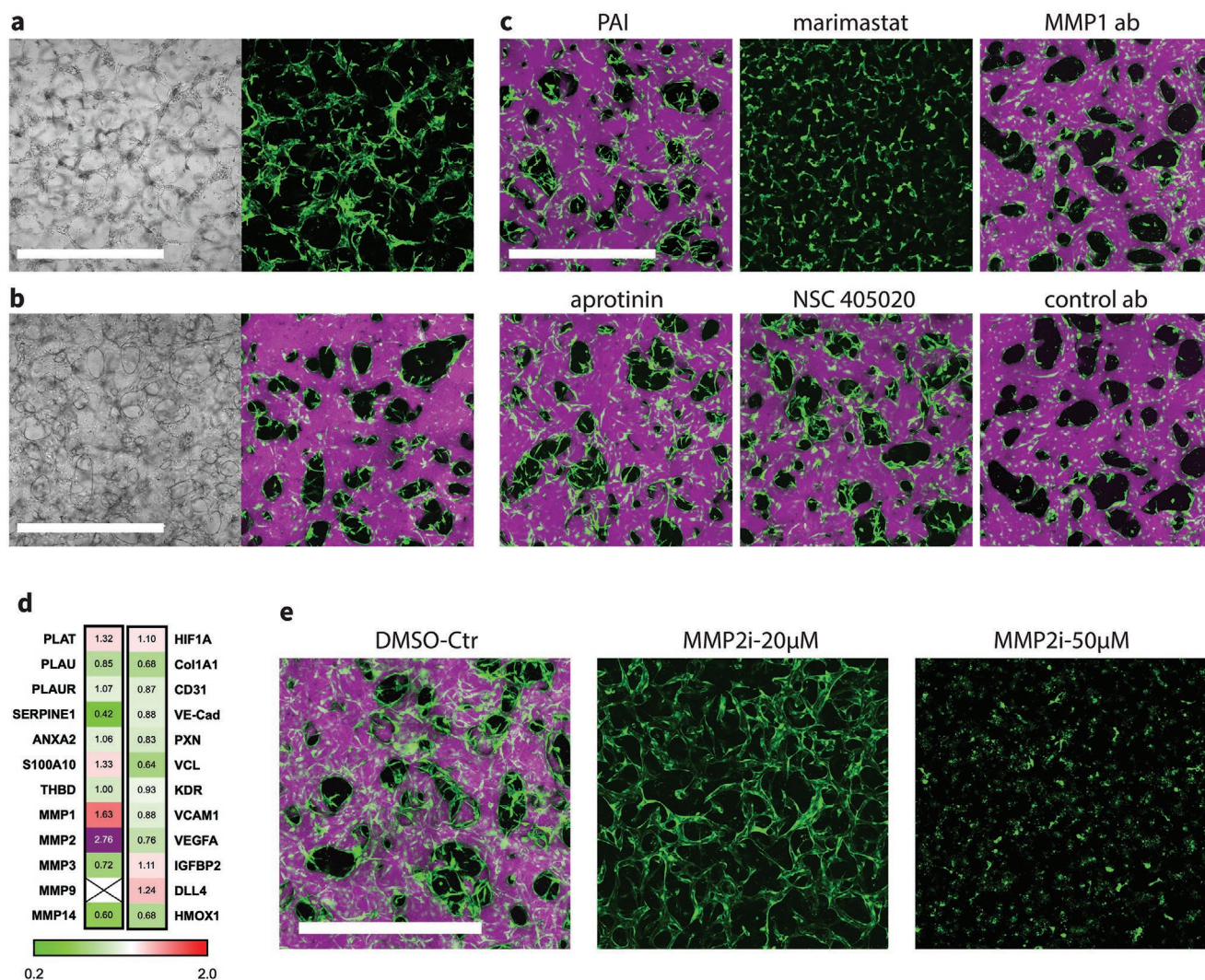


Figure 4. IF enhances the vasculogenesis ability of ECs through upregulation of MMP-2. a) MVNs formed statically with HUVEC monoculture in the three-channel device. Scale bar is 1 mm. b) MVNs formed with HUVEC monoculture in single-channel device under IF induced by 10 mm H₂O pressure difference. Scale bar is 1 mm. c) MVNs formed with HUVEC monoculture under IF induced by 10 mm H₂O pressure difference, with various inhibitors added from day 0, including 100 $\times 10^{-6}$ m PAI-1, 200 U mL⁻¹ aprotinin, 50 $\times 10^{-6}$ m marimast, 50 $\times 10^{-6}$ m NSC 405020, 100 μ g mL⁻¹ MMP-1 neutralizing antibody or 100 μ g mL⁻¹ isotype control antibody. Scale bar is 1 mm. d) Fold change between HUVEC monoculture grown under IF static conditions for various genes of interest. Cross means not detected. Samples were pooled at day 2. $n = 3$, with mean value displayed in the panel. e) MVNs formed with HUVEC monoculture under IF, subjected to various concentrations of MMP-2 inhibitor ARP-100. Scale bar is 1 mm.

connected perfusable MVNs still robustly formed with similar morphology and perfusability as in the control case. Similarly, inhibiting MMP-14 did not induce any noticeable changes in formed MVNs.

Unlike MMP-1 or MMP-14, MMP-2, which is also the most upregulated MMP under IF, turns out to be crucial for vasculogenesis in fibrin scaffolds. Supplementing with 20 $\times 10^{-6}$ m of MMP-2 specific inhibitor ARP-100 significantly altered the morphology of MVNs formed with HUVEC monoculture under IF. HUVECs were only able to self-organize into MVNs with extremely narrow vessels that were not perfusable (Figure 4e). With even higher concentrations of ARP-100 (50 $\times 10^{-6}$ m), HUVECs barely migrated in the 3D gel scaffold due to the strong suppression of MMP-2 activity (Figure 4e). At day 5, most HUVECs were still not able to connect with their

neighboring cells, leading to complete failure in developing a network structure.

Since it has also been reported that hypoxia promotes the production of MMP and enables cluster-based vasculogenesis of endothelial progenitor cells,^[25] we further evaluated HIF1A with qPCR. Similar gene expression levels of HIF1A were found in MVNs cultured statically and under IF (Figure 4d), confirming that the observed enhancement in vasculogenesis in ECs cultured under IF is not induced by hypoxia.

Thus, we find that MVNs can robustly form using HUVECs alone in the presence of IF. Through qPCR measurement and a series of inhibitory tests, we further showed that HUVEC self-organize into functional MVNs in fibrin scaffolds in a plasmin independent manner. Finally, we demonstrated that IF treatment significantly enhances vasculogenesis capacity

through upregulation of a specific member of the MMP family, MMP-2.

2.5. Regulating Morphology of MVNs through Interplay between IF and MMP-2 Inhibitor while Maintaining Functionality

Concentration of MMP-2 specific inhibitor was observed to influence distinct behaviors of HUVECs for the entire duration of in vitro vessel formation (images captured at day 1, 3, and 5 under 10 , 20 , and 50×10^{-6} M ARP-100 can be found in Figure S2, Supporting Information). Inspired by the observation that MMP-2 inhibitor noticeably altered MVNs formed using HUVEC monoculture under IF in a dose-dependent manner (Figure 5a), we hypothesized that balancing MMP-2 activity through interplay between IF and MMP-2 inhibitor could be potentially used to regulate critical morphological parameters while maintaining the perfusability of engineered MVNs. Using MVNs developed by HUVEC monoculture under IF, we indeed found that appropriate concentration (10×10^{-6} M ARP-100 in this case) of MMP-2 inhibitor effectively reduced the ECM remodeling capacity of HUVECs, leading to the formation of MVNs with significantly narrower vessels, reduced coverage area, and increased branches, compared with MVNs in the control group (Figure 5b–d). Most importantly, unlike supplementing with higher dose of MMP-2 inhibitor, perfusability of MVNs treated with 10×10^{-6} M MMP-2 inhibitor are well maintained (Figure 5e). We further validated this approach using HUVEC and HLF coculture, which is probably the most common combination used to engineer functional MVNs in vitro (Figure 5f). Again, a clear dose-dependent effect of MMP-2 inhibitor was observed, following the same trend as we characterized in MVNs formed with HUVEC monoculture (Figure 5g–j). However, MVNs formed by HUVEC and HLF coculture can maintain high perfusability with a higher concentration (20×10^{-6} M ARP-100) of MMP-2 inhibitor when cultured under the same IF.

Since vascular permeability is another critical aspect regarding functionality of engineered MVNs, we measured and compared vascular permeability using media containing 40 kDa dextran under various conditions in which perfusable vessels can be robustly formed (Figure S5, Supporting Information). Interestingly, we found no clear difference in vascular permeability across all the conditions (Figure 5k), despite the MVNs exhibiting distinct morphologies. Moreover, all the measurements were on the order of 10^{-8} cm s⁻¹, comparable to vascular permeability measured in vivo using a 40 kDa dextran.^[26] These results suggest perfusable MVNs formed under various conditions in this study exhibit normal barrier functions, even those formed without supporting fibroblasts. This contrasts with previous reports that MVNs formed by HUVEC monoculture are more permeable than those formed with various types of stromal cell.^[19] The excellent barrier function of MVNs formed by HUVEC monoculture under IF cannot be explained alone by our findings regarding MMP-2 upregulation under IF, and there are likely to be other pathways working synergistically. We further compared gene expression levels in connection with ECM secretion, cell migration, adhesion, and angiogenesis on HUVECs seeded in devices cultured under static and IF conditions at day 2. However, none of those genes

were obviously upregulated by IF treatment (Figure 4d), suggesting that further evaluation on a more extensive gene library is needed in the future.

Next, we assessed the longevity of MVNs developed with HUVEC monoculture under IF with or without MMP2 inhibitor. Surprisingly, these monoculture MVNs remained perfusable from day 5 until at least day 26 when the experiment was terminated (Figure S3, Supporting Information). During this entire time, MVN morphologies only moderately changed, while vascular permeabilities were well maintained. It should be noted that IF cannot be maintained after MVNs become fully perfusable; as mentioned above, luminal flow will take over IF and lead to rapid equilibration of the pressure difference between inlet and outlet. The mechanisms responsible for this superior longevity of MVNs formed under IF remain to be investigated.

Taken together, perfusable MVNs formed with HUVEC monoculture under IF exhibit outstanding functionality in terms of perfusability, permeability and longevity. Moreover, some critical morphological parameters of the self-organized MVNs can be robustly regulated through an interplay between IF and MMP-2 inhibitor, with functionality well maintained.

2.6. IF Enhances Formation of Fully Perfusable Brain Microvascular Networks

To validate that our findings and methods are generalizable and can be used to boost the formation of other organotypic MVN models, we investigated the effect of IF treatment on vasculogenesis of an in vitro BBB model consisting of brain endothelial cells (BECs), brain pericytes (PCs), and astrocytes (ACs) that we had previously developed.^[27] In static condition, BECs self-organized into MVNs with extremely narrow vessels by day 6 (Figure 6a). Those vessels appeared to lack continuous patent lumens, which was evidenced by failed dextran perfusion. We then seeded the triculture in a single-channel device and applied IF. Consistent with our other experiments, BECs developed into a fully perfusable MVN and exhibited excellent barrier function (Figure 6d). IF also drastically altered the morphology of brain MVNs, significantly increasing vessel diameters leading to substantially perfusable networks, following the same trend we found in HUVEC-HLF experiments (Figure 6b,c). When cultured without IF, we observed perfusable vessels only rarely. In contrast, all MVNs treated with IF were fully perfusable, further validating the effectiveness of IF in forming functional MVNs in vitro (Figure 6c). Immunostaining revealed that PCs and ACs reside in the interstitial space surrounding microvessels formed by BECs in both static and IF conditions (Figure 6e,f). PCs and ACs were in direct contact with endothelium, like described in other similar brain MVN models.^[16,19] Quantitative PCR was further performed on BECs isolated from the triculture within a fibrin gel at day 2 during neovessel formation to evaluate gene levels of MMP-2. We confirmed that MMP-2 expression was increased (1.7 ± 0.26 fold) under IF, consistent with what we found in MVNs formed with HUVECs, suggesting that IF triggers the same downstream effect in both cases among different types of ECs.

Finally, we tested whether MMP-2 specific inhibitor can be employed in the brain MVN model to antagonize the effect

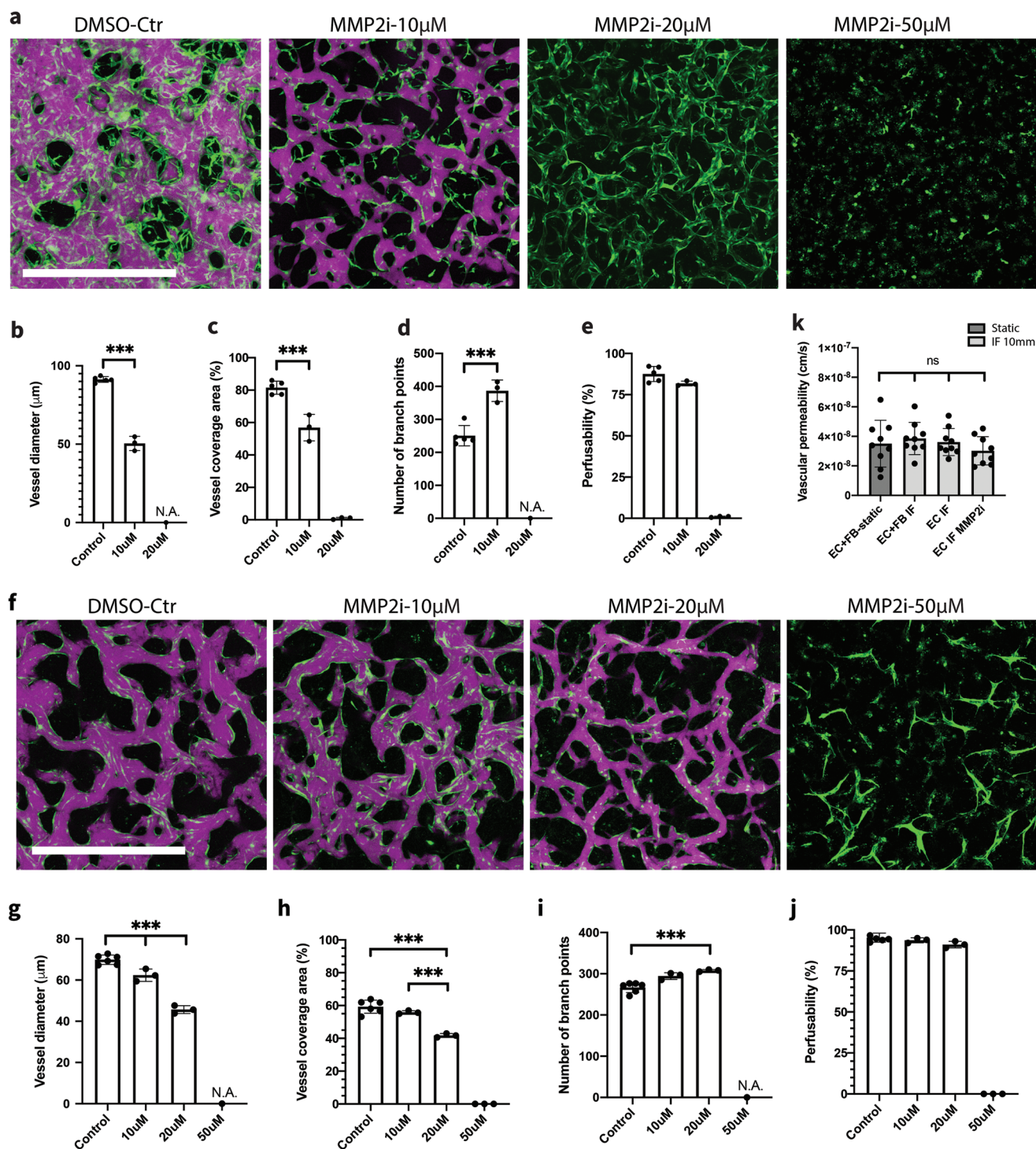


Figure 5. Regulating morphology of MVNs through interplay between IF and MMP-2 inhibitor. a) MVNs formed with HUVEC monoculture under IF, subjected to various concentrations of ARP-100. Scale bar is 1 mm. b–e) Statistical analysis of morphological parameters and perfusability of vessels cultured with various concentrations of ARP-100. IF induced by 10 mm H₂O pressure difference were applied to all cases. $n = 5$ devices for control, $n = 3$ devices for each inhibitor treated group. Significance was calculated with t -tests. $***P < 0.01$. f) MVNs formed with HUVEC-HLF coculture under IF, subjected to various concentrations of ARP-100. Scale bar is 1 mm. g–j) Statistical analysis of morphological parameters and perfusability of vessels cultured with various concentrations of ARP-100. $n = 6$ devices for control, $n = 3$ devices for each inhibitor treated group. Significance was calculated with t -tests. $***P < 0.01$. k) Vascular permeability measurements of 40 kDa dextran for perfusable MVNs formed under various conditions. $n = 3$ devices for each group, three measurements performed in each device at different ROIs.

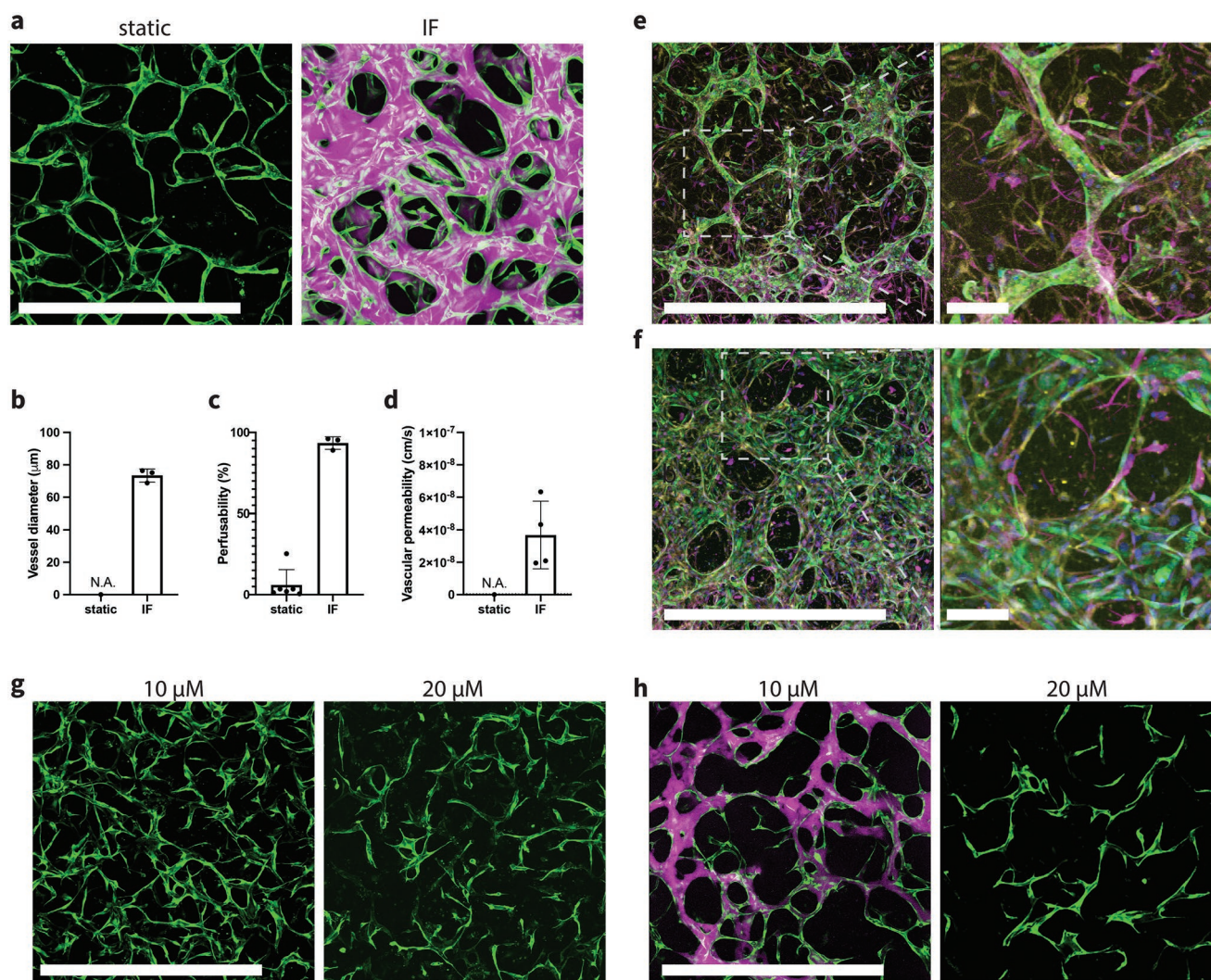


Figure 6. IF enhances formation of fully perfusable brain MVNs. a) Brain specific MVNs formed statically or under IF induced by 10 mm H₂O pressure difference. Green: GFP BECs, magenta: 40 kDa Texas Red dextran. Scale bar is 1 mm. b,c) Statistical analysis of vessel diameter and perfusability of brain MVNs formed statically or under IF. $n = 6$ devices for static group; $n = 3$ devices for IF group. d) Vascular permeability measurements using 40 kDa dextran. $n = 2$ devices, two measurements in each device at different ROIs. e) Fluorescent confocal images of brain specific MVNs cultured statically at day 6 with zoomed-in view. f) Fluorescent confocal images of brain specific MVN cultured under IF induced by 10 mm H₂O pressure difference at day 6, with zoomed-in view. Green: GFP BECs, magenta: S-100b staining for ACs, yellow: PDGFR staining for PCs. Scale bar is 1 mm for the left panel, and 100 μm for expanded view. g) Day 3 brain MVNs cultured under IF, supplemented with 10 or 20 $\times 10^{-6}$ M ARP-100. Scale bar is 1 mm. h) Day 6 brain MVNs cultured under IF, supplemented with 10 or 20 $\times 10^{-6}$ M ARP-100. Green: GFP BECs, magenta: 40 kDa Texas Red dextran. Scale bar is 1 mm.

induced by IF. Obvious differences were observed during brain MVN formation. On day 3, a higher concentration of MMP-2 inhibitor (20 $\times 10^{-6}$ M) led to thinner and sparser vessels compared with the ones treated with a lower concentration (10 $\times 10^{-6}$ M) (Figure 6g). At day 6, brain MVNs with a low concentration of MMP-2 inhibitor became perfusable with much thinner vessels compared to untreated ones. In contrast, networks cultured with the higher concentration of MMP-2 inhibitor exhibited disconnected thin network segments with no perfusable vessels (Figure 6h).

3. Discussion

Self-organized in vitro MVNs are now widely utilized as models or platforms to study development, diseases as well as basic

physiological processes, and demonstrate considerable potential in drug screening and development. Various hydrogels have been employed as a 3D scaffold to accommodate engineered MVNs, including natural materials ranging from fibrin, collagen and Matrigel to synthetic biocompatible materials such as PEG and its derivatives.^[28] Among these, fibrin is the most widely used to engineer self-organized MVNs. Understanding the dynamics between seeded ECs and fibrin ECM promises to provide valuable insight regarding the mechanism of vasculogenesis and engineering better synthetic ECM supporting formation of functional MVNs in vitro. Moreover, it could also inspire new strategies to regulate self-organizing in vitro vasculogenesis to have a degree of control over morphological parameters and perfusability in a much more robust manner. Interestingly, we found that inhibiting the PA–plasmin system, the most common means of inducing fibrinolysis, had little

effect on vasculogenesis in fibrin scaffolds. Further investigation revealed that MMP-2, a specific member of the MMP family that we found to be upregulated by applying IF, plays a critical role during the neovessel formation of engineered MVNs. Our findings are consistent with previous reports that EC invasion and capillary morphogenesis in fibrin were not affected by plasmin inhibitors, and in contrast, these processes were completely inhibited by natural and synthetic MMP inhibitors.^[20,22,23]

A simple single-channel device was fabricated to grow MVNs under IF. We extensively characterized the IF with both experiments and computations to ensure that a relatively stable IF could be maintained during neovessel formation. With this approach, we then systematically investigated the effect of IF on engineered MVNs and found that IF significantly affects neovessel formation, leading to MVNs with larger and more uniform diameters compared with those cultured under static conditions. As a consequence, perfusability, a crucial attribute of engineered MVNs, was dramatically improved. Further PCR analysis and a series of carefully designed inhibitory tests directly relate IF treatment with MMP-2 activities of ECs. MVNs cultured under IF responded in a dose-dependent manner when subjected to various concentrations of MMP-2 specific inhibitor. With a suitable dose, we are able to balance MMP-2 activity through the interplay between IF and MMP-2 inhibitor, to obtain MVNs with small diameter but still fully perfusable vessels. This method has been successfully used in the current study to produce such vessels in generic MVNs using HUVEC monoculture or HUVEC-HLF coculture (Figure 4), and BBB models with triculture of BECs, PCs, and ACs (Figure 5). Furthermore, although the geometry of spontaneously formed MVNs cannot be predefined, our methodology confers a certain level of control over many important morphological parameters during self-organized neovessel formation, thereby enabling production of MVNs with desired morphology for various applications.

Although we identified MMP-2 as the major downstream effector responsible for enhanced vasculogenesis capacity of ECs when cultured under physiologically relevant IF, the detailed underlying mechanism is currently under further investigation. We hypothesize this IF-mediated response involves signaling at cell–matrix interfaces: IF leads to clustering of corresponding integrins through activation of focal adhesion kinase (FAK), which further induces elevated metalloproteinase expression, thus allowing rapid and robust vascular network formation. Our hypothesis is well supported by several relevant works. For example, it has been shown that fluid shear stress results in increased FAK/Src phosphorylation and integrin clustering.^[29,30] Furthermore, FAK participates in recruitment of vinculin and the formation of large focal adhesions that lead to the upregulation of MMPs, thereby enabling the cell sprouting and migration necessary for vascular morphogenesis.^[31]

Proper barrier function is an essential aspect of functional MVNs. Measurements of vascular permeability were thus carried out on various MVNs formed under different conditions with 40 kDa fluorescent dextran. Excellent barrier function was demonstrated with our measurements (permeability $\approx 10^{-8}$ cm s⁻¹), which was shown to be up to two orders of magnitude lower

than that measured in static transwell cultures and comparable to values measured in vivo.^[26] No noticeable differences in vascular permeability were observed between MVNs cultured statically or under IF, suggesting IF could be employed as a robust method to boost perfusability of engineered MVNs without weakening barrier function. During those experiments, we find our single-channel device is ideal for vascular permeability measurement. The long gel region eliminates contamination from free diffusion of dextran through porous hydrogel, which is an issue for the typical three-channel design and some commercial MVN chips. Also because of the large gel region and the application of IF, the length of the perfusable MVNs formed is 1.5 cm, one order of magnitude larger than typical self-organized MVNs formed statically. Our approach might therefore be useful in engineering large-scale vascularized bulk tissues by vascular self-assembly and applied more broadly in various applications combined with IF.

In most microfluidic chips, maintaining a homogenous stable IF during neovessel formation is quite challenging, even with the help of pumping system sometimes. To test if our approach can be broadly applied to boost formation of fully perfusable MVNs, we employed same setup to establish pressure gradient in commonly used three-channel device by hooking syringes in four media reservoirs (Figure S4a, Supporting Information). Due to the small width of the gel region (3 mm), the pressure gradient rapidly dissipates. Our simulation confirmed IF speed decreases 50% in about 2.5 h after the initial pressure difference is established (Figure S4b, Supporting Information). However, this transient IF still sufficiently boosted the formation of fully perfusable MVNs with HUVEC monoculture (Figure S4c, Supporting Information), similar to MVNs cultured under relatively stable IF. Furthermore, we confirmed applying IF at a later time point could rescue defective MVNs and make it perfusable. MVNs cultured statically for 3 d using HUVEC monoculture exhibited abnormal morphologies of disconnected narrow vascular segments. Morphology of the MVNs gradually improved after applying transient IF from day 3, and eventually the network became perfusable at day 9 (Figure S4d, Supporting Information).

Recent years have seen explosive growth in the number and variety of engineered MVNs using various sources of ECs and stromal cells to mimic specific in vivo vascular microenvironments. It is now widely recognized, however, that different types of ECs, or even a single type of ECs but from different donors, often exhibit widely divergent levels of vascular morphology and perfusability. Our approach thus offers the potential to confer vessel-forming capacity among cells from various sources in order to ensure robust formation of functional MVNs. Specifically, our methodology can be used to boost the formation of certain organotypic MVNs that are difficult to form, or not yet available, saving tremendous time and resources. Moreover, MVNs are often engineered to study interactions with other physiological systems, such as neural or muscular tissues, or used as a platform to host various developing organoids.^[32–36] In those multiculture systems, the choice of hydrogel scaffold and composition of culture medium must be carefully designed to support the development and growth of all the cellular components. With our methodology, MVN development in multiculture systems could be substantially improved by employing

IF to boost vasculogenesis, significantly broadening the application of self-organized MVNs.

4. Conclusion

We systematically investigated the effect of IF on neovessel formation of self-organized MVNs in vitro using a customized single-channel device, for which IF was fully characterized. Gene expression analysis and inhibitory tests revealed that the vasculogenic capacity of ECs induced by IF results from upregulation of MMP-2. Balancing MMP-2 activity through the interplay between IF and an MMP-2 specific inhibitor, we managed to regulate many key morphological parameters of self-organized MVNs, while maintaining vascular permeability, perfusability and longevity. Our findings were further validated with an organ-specific MVN (brain) comprised of BECs, PCs and ACs, demonstrating that the identified mechanism and proposed methodology can be utilized to promote the formation of various functional MVNs with broad applications.

5. Experimental Section

Device Design and Fabrication: Two types of microfluidic device were made for this study: i) a three-channel device, featuring a central gel channel and two adjacent medium channels for culturing MVNs under static conditions (Figure 1a). A partial wall separates the central gel channel and side medium channels, allowing for surface-tension-assisted filling of cell-laden fibrin gels. ii) A single-channel device for growing MVNs under various IF conditions (Figure 1b). Single-channel devices consist of two layers: a bottom layer with a single gel channel and a top layer with larger holes at inlet and outlet. Molds of the devices were designed in AutoCAD (Autodesk, Inc.), and imported in Fusion 360 (Autodesk, Inc.) to generate corresponding tool paths, followed by milling a delrin block with a micro-CNC milling machine (Bantam Tools). Polydimethylsiloxane (PDMS) based microfluidic devices were then fabricated using the procedure outlined previously.^[27] For single-channel devices, 2 mm holes for the gel injection ports were punched in bottom layer, and 4 mm holes at inlet and outlet on top layer for attaching syringes to establish various IFs.

Cell Culture: HUVECs and normal HLFs (Lonza) were cultured in Vasculife VEGF Endothelial Medium (Lifeline Cell Technology) and FibroLife S2 Fibroblast Medium (Lifeline Cell Technology), respectively. HUVECs were transduced to express cytoplasmic GFP, as described earlier.^[5] Primary human BECs, PCs, and ACs were purchased from ScienCell, cultured in corresponding growth medium (ScienCell) on a poly-L-lysine (Sigma) coated flask. All the cells were maintained in a humidified incubator (37 °C, 5% CO₂), with the culture medium replenished every 2 d. All cell types were used between passages 6 and 8.

Microvascular Network Formation and Establishing IF: Cells were cultured until near-confluent prior to detachment, and seeded into the chip as previously described.^[27] Briefly, cells were concentrated in Vasculife containing thrombin (4 U mL⁻¹, Sigma). Cell mixture solution was then further mixed with fibrinogen (3 mg mL⁻¹ final concentration, Sigma). The cell-laden fibrin solution was quickly injected into the device through the gel loading port. Various combinations of cells were used in this study to engineer different types of MVNs. For MVNs formed with HUVECs and HLFs, the final concentration is 7 M HUVECs mL⁻¹ and 1 M HLFs mL⁻¹. For MVNs formed with HUVEC monoculture, the final concentration is 8 M HUVECs mL⁻¹. For brain MVNs, the final concentration is 6 M BECs mL⁻¹, 1 M ACs mL⁻¹, and

0.5 M PCs mL⁻¹. After seeding, the devices were placed in incubator for 15 min to allow complete polymerization, before adding Vasculife as culture media. Using syringes (3 mL sterile luer slip tip syringe, BH Supplies), a hydrostatic pressure difference was established to generate IF across the gel in the single-channel device, which can be maintained for 24 h (Figure 1c and Supporting Information). Culture medium was replenished every 24 h to restore the pressure gradient. All devices were kept in incubator with daily change of culture media for 5–7 d, until perfusable MVNs were formed.

Measurement of Matrix and Vascular Permeability: The difference in height of culture medium in the syringes attached at the inlet and outlet drives IF through the gel region of the single-channel device. Through Darcy's law, matrix permeability from liquid volume accumulated in the outlet reservoir at a given time can be measured (for detailed analytical calculation please see the Supporting Information). Vascular permeability was measured for various perfusable MVNs engineered in this study following published protocols.^[26,27] Briefly, 40 kDa Texas red dextran (Invitrogen) was perfused into the microvascular networks by generating a slight pressure gradient across the gel of the device. Confocal images were captured with a 5 μm step size at 0 and 12 min, from which permeability was calculated (Figure S5, Supporting Information). Several regions of interest (ROIs) were captured via time-lapse volumetric imaging for each device. Dimensions of the ROI are 1.6 mm × 1.6 mm (640 × 640 pix).

Microvascular Network Perfusion, Imaging, and Analysis: To confirm the perfusability of MVNs, 40 kDa Texas red dextran solution was perfused into the microvascular networks by generating a slight pressure gradient across the gel region. Confocal images were then acquired using an Olympus FLUOVIEW FV1200 confocal laser scanning microscope with a 10× objective. Z-stack images were acquired with a 10 μm step size. Morphological parameters were analyzed and quantified based on collapsed z-stack images using AutoTube.^[18] In addition, perfusability of MVNs was calculated as the ratio between dextran projected area (perfusable vessels) and GFP ECs projected area (all the vessels), presented as a percentage. If not otherwise specified, ROIs are 4 mm × 1.6 mm (2000 × 800 pix, with stitching) and 1.6 mm × 1.6 mm (800 × 800 pix) for single-channel devices and three-channel devices, respectively.

Treatment of Inhibitors: All inhibitor experiments were performed using the single-channel device with IF induced by 10 mm H₂O pressure difference. Individual inhibitor was supplemented in the culture media for the whole duration of MVN formation. Control experiments with DMSO and corresponding isotype control antibody were also performed. The concentrations and functions of the inhibitors are as follows. Plasminogen activator inhibitor-1 (Peptrotech): 100 × 10⁻⁶ M, inhibits both uPA and tPA. Aprotinin (Millipore, #A1153-10MG): 200 U mL⁻¹, inhibits plasmin. Marimast (R&D systems): 50 × 10⁻⁶ M, broad spectrum MMP inhibitor. ARP-100 (R&D systems): 10, 20, 50 × 10⁻⁶ M, MMP-2 specific inhibitor. NSC 405020 (R&D systems): 50 × 10⁻⁶ M, selective inhibitor of MT1-MMP. Anti-MMP-1 neutralizing antibody (R&D systems, #MAB901): 100 μg mL⁻¹.

Cell Liberation from MVNs, Flow Cytometry, and RT-PCR: Gene expression levels of the MVN cell components were measured to assess changes due to IF treatment, following a published protocol.^[27] In brief, cells were isolated from devices 2 d after seeding using liberase (Sigma). Gels from three single-channel devices and three 3-channel devices were pooled to ensure that enough ECs can be isolated via fluorescence-activated cell sorting (FACS) to obtain suitable RNA levels necessary for appropriate gene quantification by PCR.

Corresponding HUVECs or BECs were sorted using their intrinsic GFP expressions. Total RNA was isolated using TRIzol (Life Science). Reverse transcription was performed using High-Capacity RNA-to-cDNA Kit (Thermo Fisher Scientific). TB Green Premix Ex Taq II (Takara) was used for RT-PCR, performed on a 7900HT Fast Real-Time PCR System (Applied Biosystems). Glyceraldehyde 3-phosphate dehydrogenase (GAPDH) was used as the control housekeeping gene. Primers were synthesized by Genewiz. All primers used in this study are listed in the Supporting Information.

Computational Fluid Dynamic Model: Simulation using COMSOL Multiphysics was performed to determine the IF profile in the modified single-channel device with nonuniform width of the gel region (Figure 3a,c). IF was modeled and solved by analysis of the Darcy–Brinkman equation applied over the gel region. Matrix permeability was set as the value measured for acellular fibrin gel (Figure 1d).

Immunofluorescence Staining: Brain MVNs cultured under static or IF conditions were immunostained following a published protocol.^[27] Briefly, brain MVNs cultured for 6 d were fixed in 4% paraformaldehyde (PFA, Electron Microscopy Sciences) overnight at room temperature, following by permeabilizing with 0.2% Triton X-100 (Sigma-Aldrich) and then blocking with 5% goat serum (Invitrogen). Subsequently, primary antibodies (1:200, volume ratio) against S-100b (Sigma, S2532), PDGFR (abcam, ab32570), were used to identify ACs and PCs, respectively. After washing with PBS, devices were incubated with secondary antibodies (Invitrogen, anti-rabbit Alexa Fluor 488, anti-mouse Alexa Fluor 647) overnight at 4 °C, placed on a shaker. After washing, devices were imaged using an Olympus FLUOVIEW FV1200 confocal laser scanning microscope.

Statistics: All bar plots are shown as mean ± SD and plotted with Prism (GraphPad). All data representation details are provided in corresponding figure captions. Statistical significance was assessed using *t*-test performed in Matlab (MathWorks). * denotes $p < 0.05$, *** denotes $p < 0.01$.

Supporting Information

Supporting Information is available from the Wiley Online Library or from the author.

Acknowledgements

S.Z. and Z.W. contributed equally to this work. This work was supported by the Wellcome Leap HOPE Program, NIH NCI (U54 CA261694) and NIH NINDS (R01 NS121078).

Conflict of Interest

RDK is co-founder and has financial interest in AIM Biotech, a manufacturer of microfluidic systems. He also receives research support from Novartis, Amgen, GSK, Boehringer-Ingelheim, AbbVie, and Roche.

Data Availability Statement

The data that support the findings of this study are available from the corresponding author upon reasonable request.

Keywords

blood–brain barrier, interstitial flow, matrix metalloproteinase-2, microphysiological system, microvascular networks, vasculogenesis

Received: June 14, 2022

Revised: July 20, 2022

Published online:

[1] S. Zhang, Z. Wan, R. D. Kamm, *Lab Chip* **2021**, *21*, 473.

[2] J. A. Whisler, M. B. Chen, R. D. Kamm, *Tissue Eng., Part C* **2014**, *20*, 543.

- [3] S. Kim, H. Lee, M. Chung, N. L. Jeon, *Lab Chip* **2013**, *13*, 1489.
- [4] M. L. Moya, Y. H. Hsu, A. P. Lee, C. C. Hughes, S. C. George, *Tissue Eng., Part C* **2013**, *19*, 730.
- [5] Z. P. Wan, S. Zhang, A. X. Zhong, S. E. Shelton, M. Campisi, S. K. Sundararaman, G. S. Offeddu, E. Ko, L. Ibrahim, M. F. Coughlin, T. K. Liu, J. Bai, D. A. Barbie, R. D. Kamm, *Biomaterials* **2021**, 276.
- [6] Z. P. Wan, A. X. Zhong, S. Zhang, G. Pavlou, M. F. Coughlin, S. E. Shelton, H. T. Nguyen, J. H. Lorch, D. A. Barbie, R. D. Kamm, *Small Methods* **2022**, 2200143.
- [7] E. Gordon, L. Schimmel, M. Frye, *Front. Physiol.* **2020**, *11*, 684.
- [8] S. Zhang, E. L. Kan, R. D. Kamm, *APL Bioeng.* **2022**, *6*, 030401.
- [9] S. Kim, M. Chung, J. Ahn, S. Lee, N. L. Jeon, *Lab Chip* **2016**, *16*, 4189.
- [10] Y. Abe, M. Watanabe, S. Chung, R. D. Kamm, K. Tanishita, R. Sudo, *APL Bioeng.* **2019**, *3*, 036102.
- [11] R. Sudo, S. Chung, I. K. Zervantonakis, V. Vickerman, Y. Toshimitsu, L. G. Griffith, R. D. Kamm, *FASEB J.* **2009**, *23*, 2155.
- [12] P. A. Galie, D. H. T. Nguyen, C. K. Choi, D. M. Cohen, P. A. Janmey, C. S. Chen, *Proc. Natl. Acad. Sci. USA* **2014**, *111*, 7968.
- [13] J. H. Yeon, H. R. Ryu, M. Chung, Q. P. Hu, N. L. Jeon, *Lab Chip* **2012**, *12*, 2815.
- [14] Y. Nashimoto, T. Hayashi, I. Kunita, A. Nakamasu, Y. S. Torisawa, M. Nakayama, H. Takigawa-Imamura, H. Kotera, K. Nishiyama, T. Miura, R. Yokokawa, *Integr. Biol.* **2017**, *9*, 506.
- [15] K. Haase, F. Piatti, M. Marcano, Y. Shin, R. Visone, A. Redaelli, M. Rasponi, R. D. Kamm, *Biomaterials* **2022**, *280*, 121248.
- [16] M. A. Winkelman, D. Y. Kim, S. Kakarla, A. Grath, N. Silvia, G. Dai, *Lab Chip* **2021**, *22*, 170.
- [17] M. A. Swartz, M. E. Fleury, *Annu. Rev. Biomed. Eng.* **2007**, *9*, 229.
- [18] J. A. Montoya-Zegarra, E. Russo, P. Runge, M. Jadhav, A. H. Willrodt, S. Stoma, S. F. Norrelykke, M. Detmar, C. Halin, *Angiogenesis* **2019**, *22*, 223.
- [19] M. Campisi, Y. Shin, T. Osaki, C. Hajal, V. Chiono, R. D. Kamm, *Biomaterials* **2018**, *180*, 117.
- [20] N. Hiraoka, E. Allen, I. J. Apel, M. R. Gyetko, S. J. Weiss, *Cell* **1998**, *95*, 365.
- [21] M. S. Pepper, *Arterioscler. Thromb. Vasc. Biol.* **2001**, *21*, 1104.
- [22] R. Montesano, M. S. Pepper, J. D. Vassalli, L. Orci, *J. Cell. Physiol.* **1987**, *132*, 509.
- [23] C. L. E. Helm, M. E. Fleury, A. H. Zisch, F. Boschetti, M. A. Swartz, *Proc. Natl. Acad. Sci. USA* **2005**, *102*, 15779.
- [24] T. L. Haas, *Can. J. Physiol. Pharm.* **2005**, *83*, 1.
- [25] M. R. Blatchley, F. Hall, S. Wang, H. C. Pruitt, S. Gerecht, *Sci. Adv.* **2019**, *5*, eaau7518.
- [26] G. S. Offeddu, K. Haase, M. R. Gillrie, R. Li, O. Morozova, D. Hickman, C. G. Knutson, R. D. Kamm, *Biomaterials* **2019**, *212*, 115.
- [27] C. Hajal, G. S. Offeddu, Y. Shin, S. Zhang, O. Morozova, D. Hickman, C. G. Knutson, R. D. Kamm, *Nat. Protoc.* **2022**, *17*, 95.
- [28] A. Brown, H. K. He, E. Trumper, J. Valdez, P. Hammond, L. G. Griffith, *Biomaterials* **2020**, 243.
- [29] R. H. Vera, E. Genove, L. Alvarez, S. Borros, R. Kamm, D. Lauffenburger, C. E. Semino, *Tissue Eng., Part A* **2009**, *15*, 175.
- [30] V. Vickerman, R. D. Kamm, *Integr. Biol.* **2012**, *4*, 863.
- [31] Z. Wei, R. Schnellmann, H. C. Pruitt, S. Gerecht, *Cell Stem Cell* **2020**, *27*, 798.
- [32] J. Kim, K. T. Lee, J. S. Lee, J. Shin, B. F. Cui, K. Yang, Y. S. Choi, N. Choi, S. H. Lee, J. H. Lee, Y. S. Bahn, S. W. Cho, *Nat. Biomed. Eng.* **2021**, *5*, 830.
- [33] S. Rajasekar, D. S. Y. Lin, L. Abdul, A. Liu, A. Sotra, F. Zhang, B. Y. Zhang, *Adv. Mater.* **2020**, *32*.

- [34] Y. S. Zhang, A. Arneri, S. Bersini, S. R. Shin, K. Zhu, Z. Goli-Malekabadi, J. Aleman, C. Colosi, F. Busignani, V. Dell'Erba, C. Bishop, T. Shupe, D. Demarchi, M. Moretti, M. Rasponi, M. R. Dokmeci, A. Atala, A. Khademhosseini, *Biomaterials* **2016**, *110*, 45.
- [35] F. Bonanini, D. Kurek, S. Previdi, A. Nicolas, D. Hendriks, S. de Rooter, M. Meyer, M. C. Cabrer, R. Dinkelberg, S. B. Garcia, B. Kramer, T. Olivier, H. L. Hu, C. Lopez-Iglesias, F. Schavemaker, E. Walinga, D. Dutta, K. Queiroz, K. Domansky, B. Ronden, J. Joore, H. L. Lanz, P. J. Peters, S. J. Trietsch, H. Clevers, P. Vulto, *Angiogenesis* **2022**, <https://doi.org/10.1007/s10456-022-09842-9>.
- [36] H. T. Cui, W. Zhu, Y. M. Huang, C. Y. Liu, Z. X. Yu, M. Nowicki, S. D. Miao, Y. L. Cheng, X. Zhou, S. J. Lee, Y. F. Zhou, S. N. Wang, M. Mohiuddin, K. Horvath, L. G. Zhang, *Biofabrication* **2020**, *12*.